J|A|C|S
ARTICLES
Published on Web 02/16/2008

Probing the Compound I-like Reactivity of a Bare High-Valent Oxo Iron Porphyrin Complex: The Oxidation of Tertiary Amines

Barbara Chiavarino,[†] Romano Cipollini,[†] Maria Elisa Crestoni,[†] Simonetta Fornarini,*[,†] Francesco Lanucara,[†] and Andrea Lapi[‡]

Dipartimento di Chimica e Tecnologia delle Sostanze Biologicamente Attive, Università di Roma "La Sapienza" P.le A. Moro 5, I-00185, Roma, Italy, and Dipartimento di Chimica and Istituto CNR di Metodologie Chimiche-IMC, Sezione Meccanismi di Reazione, Università di Roma "La Sapienza" P.le A. Moro 5, I-00185, Roma, Italy

Received September 20, 2007; E-mail: simonetta.fornarini@uniroma1.it

Abstract: The mechanisms of oxidative N-dealkylation of amines by heme enzymes including peroxidases and cytochromes P450 and by functional models for the active Compound I species have long been studied. A debated issue has concerned in particular the character of the primary step initiating the oxidation sequence, either a hydrogen atom transfer (HAT) or an electron transfer (ET) event, facing problems such as the possible contribution of multiple oxidants and complex environmental effects. In the present study, an oxo iron(IV) porphyrin radical cation intermediate **1**, $[(TPFPP)^{\bullet+}Fe^{IV}{=}O]^+$ (TPFPP = meso-tetrakis (pentafluorophenyl)porphinato dianion), functional model of Compound I, has been produced as a bare species. The gas-phase reaction with amines (A) studied by ESI-FT-ICR mass spectrometry has revealed for the first time the elementary steps and the ionic intermediates involved in the oxidative activation. Ionic products are formed involving ET ($A^{\bullet+}$, the amine radical cation), formal hydride transfer (HT) from the amine ($[A(-H)]^+$, an iminium ion), and oxygen atom transfer (OAT) to the amine (A(O), likely a carbinolamine product), whereas an ionic product involving a net initial HAT event is never observed. The reaction appears to be initiated by an ET event for the majority of the tested amines which included tertiary aliphatic and aromatic amines as well as a cyclic and a secondary amine. For a series of *N*,*N*-dimethylanilines the reaction efficiency for the ET activated pathways was found to correlate with the ionization energy of the amine. A stepwise pathway accounts for the C—H bond activation resulting in the formal HT product, namely a primary ET process forming $A^{\bullet+}$, which is deprotonated at the α-C—H bond forming an *N*-methyl-*N*-arylaminomethyl radical, $A(-H)^{\bullet}$, readily oxidized to the iminium ion, $[A(-H)]^+$. The kinetic isotope effect (KIE) for proton transfer (PT) increases as the acidity of the amine radical cation increases and the PT reaction to the base, the ferryl group of $(TPFPP)Fe^{IV}{=}O$, approaches thermoneutrality. The ET reaction displayed by **1** with gaseous *N*,*N*-dimethylaniline finds a counterpart in the ET reactivity of FeO^+, reportedly a potent oxidant in the gas phase, and with the barrierless ET process for a model $(P)^{\bullet+}Fe^{IV}{=}O$ species (where P is the porphine dianion) as found by theoretical calculations. Finally, the remarkable OAT reactivity of **1** with $C_6F_5N(CH_3)_2$ may hint to a mechanism along a route of diverse spin multiplicity.

Introduction

The oxidative N-dealkylation of tertiary amines is an important process, well documented in chemistry and biochemistry. In particular, it constitutes a major pathway for the disposition of xenobiotic amines including many drugs. In the biological environment the process is catalyzed by heme enzymes, notably by the peroxidase and cytochrome P450 families of enzymes,[1] and results from the formal hydroxylation of a carbon adjacent to nitrogen effected by a short-lived oxidant named Compound I and abbreviated as $(Porp)^{\bullet+}Fe^{IV}{=}O$, where Porp is the protoporphyrin IX dianion. The reaction conceivably proceeds by an unstable carbinolamine intermediate that evolves by nonenzymatic cleavage between the hydroxylated carbon and the nitrogen atom. For the enzymatic N-dealkylation reaction two mechanisms have been formulated, differing for the primary reactive step (Scheme 1).[1−3] In the first route, a single electron oxidation (ET) of the heteroatom gives a radical cation which undergoes subsequent deprotonation (PT) at a C—H bond on the carbon adjacent to the heteroatom, forming an α-carbon centered neutral radical. Alternatively, a hydrogen atom transfer (HAT) mechanism has been found to operate for example in the cytochrome P450-catalyzed oxidation of 4-substituted *N*,*N*-dimethylanilines and of *N*-cyclopropyl-*N*-alkyl-anilines.[2,3] The varied pattern of mechanistic pathways activated by cytochrome P450 and peroxidase enzymes and their model compounds is recognized to depend on the chemical and electronic structures

[†] Dipartimento di Chimica e Tecnologia delle Sostanze Biologicamente Attive.
[‡] Dipartimento di Chimica and Istituto CNR di Metodologie Chimiche-IMC.

10.1021/ja077286t CCC: $40.75

Scheme 1. Proposed Mechanisms in Oxidative N-Demethylation of Tertiary Amines Catalyzed by $(Porp)^{\bullet+}Fe^{IV}{=}O$, Initiated by Either H-Atom Abstraction (HAT) or Single Electron Transfer (ET)

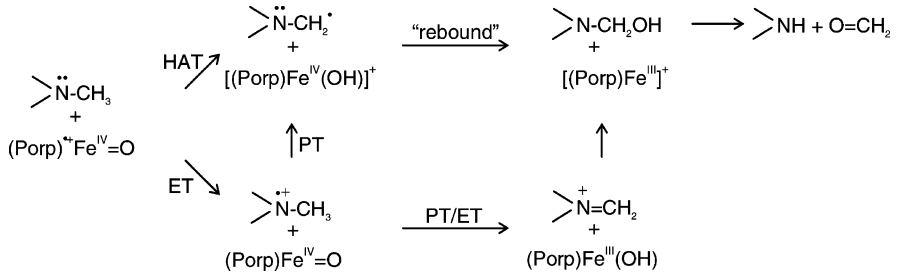

of substrates and active catalytic species that may affect the partition between competitive routes.[1,4,5] However, in spite of intense interest in the past two decades, not all ambiguities have been solved and there is a clear need for further work.[1,6] In particular, the direct observation of the significant steps in the oxidation process is crucial for the elucidation of the detailed mechanism. This is the aim of the present work, providing a close, direct view of the charged intermediates involved in the oxidation of gaseous amines by a synthetic oxo iron(IV) porphyrin π-cation radical used as chemical model of the Compound I intermediate.

In the study of complex reaction mechanisms that involve the formation and decay of transient ionic intermediates, the tools of gas-phase ion chemistry have proven valuable. In a highly dilute environment reactive intermediates are isolated and may be characterized about their structures, spectroscopic properties, reactivities, and energetics.[7] In this way a vast amount of information on gaseous metal ion complexes has been accessed and detailed insight into patterns of their catalytic activity has been obtained.[8] The advent of electrospray ionization (ESI)[9] coupled to mass spectrometry (MS) has added a new dimension to the potential information that can be gathered from the gas-phase chemistry of metal ion complexes.[10] Ionic species in dilute solution can be transferred intact directly to the gas phase. One can take advantage of ESI-MS to isolate postulated intermediates and investigate their reactivity patterns in the gas phase, also relying on the remarkable similarity that is frequently observed between ion molecule reactions in the gas phase and the corresponding solution-phase reactions.[10]

In a recent report, a model of the high-valent oxo iron(IV) species that is invoked as the key intermediate in enzymatic oxygenation reactions has been produced and studied as a naked ion in the gas phase.[11] The oxo iron(IV) porphyrin radical cation intermediate **1**, $[(TPFPP)^{\bullet+}Fe^{IV}{=}O]^+$ (where TPFPP is a 5,10,-15,20-tetrakis(pentafluorophenyl)porphinato dianion and the whole species within square brackets owns a unit positive charge), was prepared by the reaction of the iron(III) porphyrin chloride, $(TPFPP)Fe^{III}Cl$, with H_2O_2 in methanol and transferred to the gas phase under mild ESI conditions. The elementary steps of its gas-phase reaction with simple molecules of biological significance (L) have been studied by FT-ICR mass spectrometry providing data on intrinsic reactivity features and on the formation of transient intermediates. The bare $[(TPFPP)^{\bullet+}Fe^{IV}{=}O]^+$ ion (**1**) is found to react by oxygen atom transfer to L (eq 1a), releasing $[(TPFPP)Fe^{III}]^+$, and by addition (eq 1b), yielding $[(TPFPP)Fe(L)O]^+$. While it behaves as a sluggish

(1) (a) Ortiz de Montellano, P. R. *Cytochrome P450: Structure, Mechanism and Biochemistry*, 3rd ed.; Kluwer Academic/Plenum Publishers: New York, 2005. (b) Guengerich, F. P. *Chem. Res. Toxicol.* **2001**, *14*, 611. (c) Groves, J. T. *J. Inorg. Biochem.* **2006**, *100*, 434. (d) Groves, J. T. *Proc. Natl. Acad. Sci. U.S.A.* **2003**, *100*, 3569. (e) Sono, M.; Roach, M. P.; Coulter, E. D.; Dawson, J. H. *Chem. Rev.* **1996**, *96*, 2841. (f) Loew, G. H.; Harris, D. L. *Chem. Rev.* **2000**, *100*, 407. (g) Meunier, B.; de Visser, S. P.; Shaik, S. *Chem. Rev.* **2004**, *104*, 3947. (h) Shaik, S.; Kumar, D.; de Visser, S. P.; Altun, A.; Thiel, W. *Chem. Rev.* **2005**, *105*, 2279. (i) Denisov, I. G.; Makris, T. M.; Sligar, S. G.; Schlichting, I. *Chem. Rev.* **2005**, *105*, 2253. (j) Ortiz de Montellano, P. R.; De Voss, J. J. *Nat. Prod. Rep.* **2002**, *19*, 477. (k) Kim, D.; Guengerich, F. P. *Ann. Rev. Pharmacol. Toxicol.* **2005**, *45*, 27.

(2) (a) Bhakta, M. N.; Hollenberg, P. F.; Wimalasena, K. *J. Am. Chem. Soc.* **2005**, *127*, 1376. (b) Bhakta, M. N.; Hollenberg, P. F.; Wimalasena, K. *Chem. Commun.* **2005**, 265. (c) Bhakta, M. N.; Wimalasena, K. *J. Am. Chem. Soc.* **2002**, *124*, 1844. (d) Bhakta, M. N.; Wimalasena, K. *Eur. J. Org. Chem.* **2005**, 4801.

(3) (a) Karki, S. B.; Dinnocenzo, J. P.; Jones, J. P.; Korzekwa, K. R. *J. Am. Chem. Soc.* **1995**, *117*, 3657. (b) Dinnocenzo, J. P.; Karki, S. B.; Jones, J. P. *J. Am. Chem. Soc.* **1993**, *115*, 7111. (c) Shaffer, C. L.; Morton, M. D.; Hanzlik, R. P. *J. Am. Chem. Soc.* **2001**, *123*, 8502. (d) Shaffer, C. L.; Harriman, S.; Koen, Y. M.; Hanzlik, R. P. *J. Am. Chem. Soc.* **2002**, *124*, 8268. (e) Cerny, M. A.; Hanzlik, R. P. *J. Am. Chem. Soc.* **2006**, *128*, 3346. (f) Manchester, J. I.; Dinnocenzo, J. P.; Higgins, L.; Jones, J. P. *J. Am. Chem. Soc.* **1997**, *119*, 5069.

(4) (a) Watanabe, Y. In *The Porphyrin Handbook*; Kadish, K. M., Smith, K. M., Guilard, R., Eds.; Academic Press: San Diego, 2000; Vol. 4, Chapter 30, p 97. (b) Meunier, B.; Robert, A.; Pratviel, G.; Bernardou, J. In *The Porphyrin Handbook*; Kadish, K. M., Smith, K. M., Guilard, R., Eds.; Academic Press: San Diego, 2000; Vol. 4, Chapter 31, p 119. (c) Montanari, F.; Casella, L. *Metalloporphyrins Catalyzed Oxidations*; Kluwer Academic Publishers: Dordrecht, The Netherlands, 1994. (d) Fujii, H. *Coord. Chem. Rev.* **2002**, *226*, 51.

(5) (a) Baciocchi, E.; Lanzalunga, O.; Lapi, A.; Manduchi, L. *J. Am. Chem. Soc.* **1998**, *120*, 5783. (b) Baciocchi, E.; Lapi, A. *Tetrahedron Lett.* **1999**, *40*, 5425. (c) Baciocchi, E.; Gerini, M. F.; Lanzalunga, O.; Lapi, A.; Lo Piparo, M. G.; Mancinelli, S. *Eur. J. Org. Chem.* **2001**, 2305. (d) Goto, Y.; Watanabe, Y.; Fukuzumi, S.; Jones, J. P.; Dinnocenzo, J. P. *J. Am. Chem. Soc.* **1998**, *120*, 10762. (e) Lindsay Smith, J. R.; Mortimer, D. N. *J. Chem. Soc., Perkin Trans. 2* **1986**, 1743. (f) Baciocchi, E.; Gerini, M. F.; Lanzalunga, O.; Lapi, A.; Mancinelli, S.; Mencarelli, P. *Chem. Commun.* **2000**, 393. (g) Baciocchi, E.; Bietti, M.; Gerini, M. F.; Lanzalunga, O. *J. Org. Chem.* **2005**, *70*, 5144.

(6) (a) Nehru, K.; Seo, M. S.; Kim, J.; Nam, W. *Inorg. Chem.* **2007**, *46*, 293. (b) Nam, W. *Acc. Chem. Res.* **2007**, *40*, 522.

(7) (a) Nibbering, N. M. M. *Int. J. Mass Spectrom.* **2000**, *200*, 27. (b) DePuy, C. H. *J. Org. Chem.* **2002**, *67*, 2393. (c) Kass, S. R.; Broadus, K. M. *J. Phys. Org. Chem.* **2002**, *15*, 461. (d) Olmstead, W. N.; Brauman, J. I. *J. Am. Chem. Soc.* **1977**, *99*, 4219. (e) Caldwell, G.; Magnera, T. F.; Kebarle, P. *J. Am. Chem. Soc.* **1984**, *106*, 959. (f) Morton, T. H. *Tetrahedron* **1982**, *38*, 3195.

(8) (a) Rodgers, M. T.; Armentrout, P. B. *Acc. Chem. Res.* **2004**, *37*, 989. (b) Armentrout, P. B.; Beauchamp, J. L. *Acc. Chem. Res.* **1989**, *22*, 315. (c) *Organometallic Ion Chemistry*; Freiser, B. S., Ed.; Kluwer: Dordrecht, 1996. (d) Bohme, D. K.; Schwarz, H. *Angew. Chem., Int. Ed.* **2005**, *44*, 2336. (e) Schroeder, D.; Schwarz, H. *Angew. Chem., Int. Ed. Engl.* **1995**, *34*, 1973. (f) Schroeder, D.; Schwarz, H. *Top. Organomet. Chem.* **2007**, *22*, 1. (g) Operti, L.; Rabezzana, R. *Mass Spectrom. Rev.* **2006**, *25*, 483.

(9) (a) Whitehouse, C. M.; Dreyer, R. N.; Yamashita, M.; Fenn, J. B. *Anal. Chem.* **1985**, *57*, 675. (b) Fenn, J. B.; Mann, M.; Meng, C. K.; Wong, S. F.; Whitehouse, C. M. *Science* **1989**, *246*, 64.

(10) (a) Chen, P. *Angew. Chem., Int. Ed.* **2003**, *42*, 2832. (b) Gerdes, G.; Chen, P. *Organometallics* **2003**, *22*, 2217. (c) Traeger, J. C. *Int. J. Mass Spectrom.* **2000**, *200*, 387. (d) Sabino, A. A.; Machado, A. H. L.; Correia, C. R. D.; Eberlin, M. N. *Angew. Chem., Int. Ed.* **2004**, *43*, 2514. (e) Bossio, R. E.; Hoffman, N. W.; Cundari, T. R.; Marshall, A. *Organometallics* **2004**, *23*, 144. (f) Schroeder, D.; Roithova, J.; Schwarz, H. *Int. J. Mass Spectrom.* **2006**, *254*, 197. (g) Trage, C.; Diefenbach, M.; Schroeder, D.; Schwarz, H. *Chem.—Eur. J.* **2006**, *12*, 2454. (h) Feng, W. Y.; Gronert, S.; Lebrilla, C. *J. Phys. Chem. A* **2003**, *107*, 405. (i) Turecek, F. *Mass Spectrom. Rev.* **2007**, *26*, 563.

(11) Crestoni, M. E.; Fornarini, S. *Inorg. Chem.* **2005**, *44*, 5379.

$$[(TPFPP)^{\bullet+}Fe^{IV}{=}O]^+ + L \;(\mathbf{1}) \rightarrow [(TPFPP)Fe^{III}]^+ + L(O) \quad (1a)$$
$$\rightarrow [(TPFPP)Fe(L)O]^+ \quad (1b)$$

oxidant toward olefins, the reactivity with phosphites, pyridines, and sulfides is pronounced and goes in parallel with the oxophilic character of the active site of L. An insight into the dynamics of the oxygen transfer reaction has been gained probing the so-formed $[(TPFPP)Fe(L)O]^+$ adduct ions by their ion−molecule reactions with a second neutral (M). Ligand addition and ligand exchange products are observed (eq 2a and 2b, respectively). In all instances, the ligand exchange reaction involves the displacement of an L(O) unit, never occurring by displacement of L (eq 2c). This result points to the formation

$$[(TPFPP)Fe(L)O]^+ + M \rightarrow [(TPFPP)Fe(L)O(M)]^+ \quad (2a)$$
$$\rightarrow [(TPFPP)Fe(M)]^+ + L(O) \quad (2b)$$
$$\not\rightarrow [(TPFPP)Fe(M)O]^+ + L \quad (2c)$$

of an oxidized species, L(O), bound to an axial site in the iron coordination sphere, while the second axial coordination site remains vacant and thus susceptible to undergo ligand addition. The latter process would not be directly open to an isomeric $[(TPFPP)FeO(L)]^+$ species whereby an axial ligand L were bound in a trans relationship to the oxo iron moiety, as more explicitly indicated by the $[(TPFPP)(L)Fe{=}O]^+$ notation. Interestingly, the same reactivity is displayed by $[(TPFPP)Fe(L)O]^+$ ions extracted by ESI from a solution containing L besides the precursors of **1**. This finding suggests a common, distinct intermediate along the pathway to oxygen transfer products and provides evidence for the remarkable similarities that emerge when comparing reactivity patterns and transient intermediates occurring either in the gas phase or in solution, based on the assay of ESI formed ions. The reactivity of **1** toward neutrals such as NO and NO_2 is notably high, in line, though, with the recognized role of prosthetic heme groups in governing the biological chemistry of nitrogen oxides and in particular with a recently suggested protective action of nitric oxide toward highly oxidizing forms of heme proteins.[12]

Aiming to gain further information on the Compound I-like reactivity of high-valent oxo iron intermediates in a solvent free environment, the gas-phase reactivity of **1** with amines including *N*,*N*-dimethylanilines has been examined and is presently reported.

Experimental Section

Materials. All chemicals used in the experiments and precursors needed for the synthesis of useful substrates, including (5,10,15,20-tetrakis(pentafluorophenyl)porphinato)iron(III) chloride ($(TPFPP)Fe^{III}$-Cl), iodosobenzenediacetate, [D_2]paraformaldehyde, aniline, pentafluoroaniline, 4-fluoroaniline, 4-bromoaniline, 4-(trifluoromethyl)aniline, 4-methylaniline, and sodium borohydride, were research grade products obtained from commercial sources and used as received. Iodosylbenzene (C_6H_5IO) was prepared according to a published procedure[13] and stored at −20 °C. The ring substituted *N*,*N*-bis(dideuteriomethyl)anilines were prepared by the reaction of the corresponding anilines with [D_2]-paraformaldehyde and sodium borohydride as described in the literature.[3a,5c] These compounds were purified by preparative GLC using a 3 m column filled with Chromosorb 80/100 W-AW coated with a base deactivated polyethyleneglycol stationary phase, mounted on a Carlo Erba FRACTOVAP Mod. ATC/f series 410 gas chromatograph. The identity and the purity of the products, besides their deuterium content, were checked by GLC-MS on a Hewlett-Packard 5890 gas chromatograph connected to a model 5989B quadrupole mass spectrometer, performing the analysis on a 50 m long, 0.2 mm i.d. fused-silica capillary column, coated with cross-linked methylsilicone film.

Instrumental. All experiments were performed with a Bruker BioApex Fourier Transform ion cyclotron resonance (FT-ICR) mass spectrometer with an external Analytica of Branford Inc. ESI source. The instrument is equipped with a cylindrical infinity cell and a 4.7 T superconducting magnet. The vacuum is maintained by rotary vacuum pumps and turbomolecular pumps. Analyte solutions were infused into a 50 μm i.d. fused-silica capillary at a flow rate of 200 μL h^{-1} by a syringe pump, and ions were accumulated in an rf-only hexapole ion guide for 0.6 s. The ion population was pulsed into the ICR cell at room temperature, and the ion of interest was isolated by broad-band radio frequency pulses and exposed to a neutral reagent leaked by a needle valve at a constant pressure value, comprised in the range of 1×10^{-8}−2×10^{-7} mbar. Pressure readings were obtained from a cold cathode gauge, calibrated by using the rate constant $k = 1.1 \times 10^{-9}$ cm^3 s^{-1} for the reference reaction $CH_4^{\bullet+} + CH_4 \rightarrow CH_5^+ + CH_3^\bullet$ and corrected for different response factors.[14,15] In the mass spectra, corrections for ^{13}C isotopic contributions were effected whenever the ion of interest appeared as an isotopic cluster contaminated by the presence of adjacent or overlapping peaks from another ionic species. In particular, the correction was applied in evaluating kinetic isotope effects by the ratio of ion abundances for species involving either H or D atom loss.

Pseudo-first-order-rate constants were obtained from the slope of the semilog decrease of the reactant ion signal vs time and divided by the known pressure of the neutral to derive bimolecular rate constants (k_{exp}). The rate constants, obtained as average values from at least three determinations at different neutral pressures at a room temperature of 300 K, were also expressed as percentages (ϕ, namely the reaction efficiency) of the collision rate constant (k_{coll}) calculated by the parametrized trajectory theory.[16] The reproducibility of k_{exp} values was within 10%, while the error of the absolute rate constants is estimated to be ±30%. Branching ratios for parallel reaction channels were obtained by extrapolation of product ion intensities at initial times, in order to minimize any interference due to possible consecutive processes. Collision induced dissociation (CID) experiments were made in the FT-ICR cell, and argon was admitted by a pulsed valve and used as a collision gas. Isolated ions were translationally excited by an on-resonance radio frequency pulse. The excited ions were allowed to collide with argon and dissociate for as long as 5 s before the product ion radio frequency sweep.

Computational Details. DFT calculations were performed with the Spartan'04 program package (Wavefunction, Inc., Irvine, CA) at the B3LYP level (unrestricted formalism for open-shell systems) using the 6-311+G** basis set.

The reported energies include the zero-point vibrational energy, calculated at the same level. The frequency calculations also verified that the structures represented true minima. The bond dissociation energies (BDEs) were calculated using the standard definition of the BDE, that is, the difference in energy between the substrate and the sum of the radical and hydrogen atom, using optimized geometries: $BDE = E(\text{radical}) + E(H) - E(\text{substrate})$. The ionization energy (IE) of a substrate (S) and the proton affinity (PA) of a base (B) at 0 K

(12) (a) Scheidt, W. R.; Ellison, M. K. *Acc. Chem. Res.* **1999**, *32*, 350. (b) Gorbunov, N. V.; Osipov, A. N.; Day, B. W.; Zayas-Rivera, B.; Kagan, V. E.; Elsayed, N. M. *Biochemistry* **1995**, *34*, 6689. (c) Herold, S.; Rehmann, F.-J. K. *Free Radical Biol. Med.* **2003**, *34*, 269.
(13) Saltzman, H.; Sharefkin, J. G. *Organic Syntheses*; Wiley: New York, 1973; Collect. Vol. 5, p 658.
(14) Meot-Ner, M. In *Gas Phase Ion Chemistry*; Bowers, M. T., Ed.; Academic Press: New York, 1979; Vol. 1.
(15) Bartmess, J. E.; Georgiadis, R. M. *Vacuum* **1983**, *33*, 149.
(16) Su, T.; Chesnavich, W. J. *J. Chem. Phys.* **1982**, *76*, 5183.

were similarly obtained (IE = $E(S^{\bullet+}) - E(S)$ and PA = $E(B) - E(BH^+)$, where PA is defined as $-\Delta H°$ of the process: $B + H^+ \rightarrow BH^+$).

Preparation and Sampling of $[(TPFPP)^{\bullet+}Fe^{IV}=O]^+$ Ions. Preparation of the complex **1** and transfer into the gas phase have been described previously in our earlier mechanistic work on the cytochrome P450-like reactivity of high valent oxo iron intermediates in the gas phase.[11] For the present study iodosylbenzene was used as the oxidant and the pure solid was added to a 5×10^{-5} M solution of the parent $(TPFPP)Fe^{III}Cl$ complex (making a 12:1 molar ratio) in CH_3OH/CH_2Cl_2 (1:1) cooled at −40 °C. These experimental conditions result in a good compromise between a fast and efficient formation of the high-valent iron intermediate and an acceptable stability of the solution. Fresh solutions kept at −40 °C are found to be stable for about 1 h. Electrospray ionization of these solutions allows **1** to be transferred to the gas phase and finally sampled in the FT-ICR cell. Ions **1** appear in the FT-ICR mass spectrum as a prominent cluster centered at *m*/*z* 1044 (henceforth the *m*/*z* value of the dominant peak in the isotopic cluster is given). However, the overall ion signal is not totally accounted for by $[(TPFPP)^{\bullet+}Fe^{IV}=O]^+$ species because the synthetic procedure leads to a fraction of isomeric species oxidized on the porphyrin frame that cannot be removed. In order to evaluate this fraction, one can exploit the ion chemistry specific of this species. In fact, the oxidation of the porphyrin ligand, delivering an oxygen atom presumably on the porphyrin periphery or on a pyrrolic nitrogen, does not alter appreciably the reactivity of the iron center toward ligand addition. This porphyrin oxidized species reacts in a closely similar way as $[(TPFPP)Fe^{III}]^+$ ions.[11] For example, both species react with NO yielding a ligand addition product, whereas **1** releases an oxygen atom to NO.[11] Due to the easy disposal of this gaseous reagent from the FT-ICR cell, NO has thus been used to quantify the relative abundance of metal-oxidized and porphyrin-oxidized isomers, titrating[17] in this way the *m*/*z* 1044 ion population. Differences in chemical reactivity have long been recognized as a useful means for resolving isomeric ion mixtures.[18]

Results and Discussion

Synthesis and Characterization of Gaseous $[(TPFPP)^{\bullet+}Fe^{IV}=O]^+$ Ions. Obtaining a positively charged high-valent iron(IV) oxo porphyrin cation radical by a gas-phase reaction is by no means a trivial task.[11,19] Potential oxidants such as O_2, N_2O, NO_2, and oxirane were tested for reaction with $[(TPFPP)Fe^{III}]^+$ and $[(Porp)Fe^{III}]^+$; however they were found either to be unreactive (O_2, N_2O) or to lead to products other than the desired high valent oxo iron species. The synthesis of **1** was then performed in solution by controlled oxidation of $(TPFPP)Fe^{III}$-Cl. The reagent used in a previous report, H_2O_2,[11] was avoided in the present work in favor of iodosylbenzene. The reason lies in the dual reactivity of H_2O_2 which undergoes not only heterolytic cleavage, yielding **1**, but also a homolytic cleavage of the peroxidic bond leading to $[(TPFPP)Fe^{IV}(OH)]^+$.[4b,11] The gas-phase reactivity of the latter species is known to be markedly different compared with that of **1**, so that it may be expected to cause little interference with the reactivity pattern of the high valent oxo iron species under study.[11] However, because $[(TPFPP)Fe^{IV}(OH)]^+$ product ions could result from a hydrogen atom transfer process to **1**, the presence of $[(TPFPP)Fe^{IV}(OH)]^+$ in substantial amounts already in the reagent ion mixture could possibly obscure an important reaction pathway. The use of iodosylbenzene for forming high valent oxo metal complexes to be further characterized by ESI-MS is not unprecedented.[20] Exploiting this oxygen atom donor[21] is not completely void of inconveniences though. Under the adopted reaction conditions, optimizing the yield of the oxo iron complex and its lifetime in solution, the ions that appear as an isotopic peak cluster centered at *m*/*z* 1044, denote the neat addition of an oxygen atom to the reagent $[(TPFPP)Fe^{III}]^+$ ions at *m*/*z* 1028. In the ESI-FT-ICR mass spectrum (Figure 1) the two isotopic clusters of the reagent ion and the oxidized species are characterized by similar ion abundance ratios, as expected. However, when the ion cluster at *m*/*z* 1044 is isolated in the FT-ICR cell and sampled by its ion−molecule reactivity toward NO, it becomes clear that two isomeric species are present. While a major fraction of ions displays O-atom transfer reactivity, as already reported,[11] releasing $[(TPFPP)Fe^{III}]^+$ ions and NO_2 as the likely neutral product, a second, substantial fraction appears less reactive, yielding ultimately an addition product at *m*/*z* 1074. The NO ligand addition reactivity is typical of tetracoordinate $[(TPFPP)Fe^{III}]^+$ ions[11] and $[(Porp)Fe^{III}]^+$ ions[19] in the gas phase. On this basis it appears that those ions at *m*/*z* 1044 undergoing NO addition are species oxidized on the porphyrin ligand, presumably due to formation of a *N*-oxide on a pyrrole unit.[22] Figure 2 displays the time dependence of ion abundances that follow the isolation of the cluster at *m*/*z* 1044 which is then allowed to react with a stationary concentration of NO. The decay of the parent ion abundance is intrinsically biphasic, though it hardly appears so because of the close values of the time constants for the reaction of the two isomeric components. The

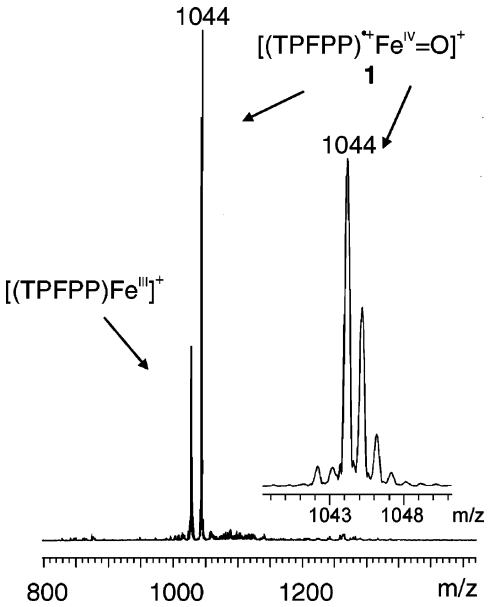

Figure 1. ESI-FT-ICR mass spectrum from a CH_3OH/CH_2Cl_2 (1:1) solution of $(TPFPP)Fe^{III}Cl$ (5×10^{-5} M) and iodosylbenzene (6×10^{-4} M). The inset shows an enlargement of the isotopic cluster at *m*/*z* 1044.

(17) (a) Bueker, H.-H.; Gruetzmacher, H.-F.; Crestoni, M. E.; Ricci, A. *Int. J. Mass Spectrom. Ion Processes* **1997**, *160*, 167. (b) Mormann, M.; Salpin, J.-Y.; Kuck, D. *Int. J. Mass Spectrom.* **2006**, *249/250*, 340.
(18) (a) McEwan, M. J. In *Advances in Gas Phase Ion Chemistry*; Adams, N., Babcock, L. M., Eds.; JAI Press: Greenwich, 1992; Vol. 1. (b) Ausloos, P.; Lias, S. G. *J. Am. Chem. Soc.* **1981**, *103*, 6505.
(19) (a) Angelelli, F.; Chiavarino, B.; Crestoni, M. E.; Fornarini, S. *J. Am. Soc. Mass Spectrom.* **2005**, *16*, 589. (b) Irikura, K. K.; Beauchamp, J. L. *J. Am. Chem. Soc.* **1991**, *113*, 2767. (c) Chen, O.; Groh, S.; Liechty, A.; Ridge, D. P. *J. Am. Chem. Soc.* **1999**, *121*, 11910. (d) Chen, O.; Hagan, S. E.; Groh, S.; Ridge, D. P. *J. Am. Chem. Soc.* **1991**, *113*, 9669.
(20) Feichtinger, D.; Plattner, D. A. *J. Chem. Soc., Perkin Trans. 2* **2000**, 1023.
(21) Groves, J. T.; Nemo, T. E.; Myers, R. S. *J. Am. Chem. Soc.* **1979**, *101*, 1032.
(22) (a) Nam, W.; Lim, M. H.; Oh, S.-Y. *Inorg. Chem.* **2000**, *39*, 5572. (b) Groves, J. T.; Watanabe, Y. *J. Am. Chem. Soc.* **1988**, *110*, 8443. (c) Machii, K.; Watanabe, Y.; Morishima, I. *J. Am. Chem. Soc.* **1995**, *117*, 6691.

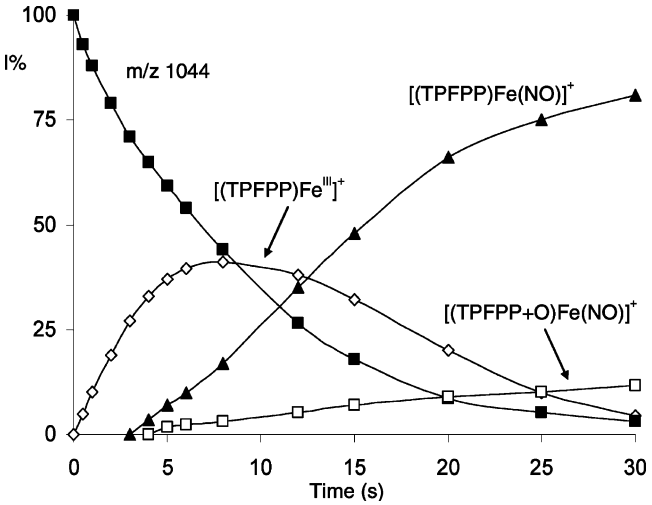

Figure 2. Time dependence of relative ion intensities (I%) following the selection of ions at *m/z* 1044 (a mixture of $[(TPFPP)^{\bullet+}Fe^{IV}{=}O]^+$ and $[(TPFPP{+}O)Fe^{III}]^+$) in the FT-ICR cell in the presence of NO at 3.8×10^{-8} mbar.

product of the oxygen atom transfer reaction, $[(TPFPP)Fe^{III}]^+$, subsequently adds NO giving $[(TPFPP)Fe^{III}(NO)]^+$ at *m/z* 1058 (eq 3a). In the slower process, the isobaric porphyrin oxidized species, henceforth depicted as $[(TPFPP{+}O)Fe^{III}]^+$, yields the NO adduct at *m/z* 1074 (eq 3b).

$$\underset{m/z\ 1044}{[(TPFPP)^{\bullet+}Fe^{IV}{=}O]^+} + NO \longrightarrow \xrightarrow{-NO_2} \underset{m/z\ 1028}{[(TPFPP)Fe^{III}]^+} \xrightarrow{+NO} \underset{m/z\ 1058}{[(TPFPP)Fe(NO)]^+} \quad (3a)$$

$$\underset{m/z\ 1044}{[(TPFPP{+}O)Fe^{III}]^+} + NO \longrightarrow \underset{m/z\ 1074}{[(TPFPP{+}O)Fe(NO)]^+} \quad (3b)$$

As a consequence of the two independent processes characterized by different rates, the ratio of the sum of ion abundances for the species at *m/z* 1028 and *m/z* 1058 relative to the sum of ion abundances for *m/z* 1044 and *m/z* 1074 ions reaches a constant value at a sufficiently long reaction time. In the experiment depicted in Figure 2 the ratio approaches the value 85:15. This constant ratio finally corresponds to the end ion abundances of $[(TPFPP)Fe^{III}(NO)]^+$ and $[(TPFPP{+}O)Fe^{III}(NO)]^+$, which do not react further with NO. The reaction with NO may then be used to probe the relative amount of the oxo iron species in each new sample solution, providing a means to titrate the relative amount of the isomer of interest in the ion population produced by ESI.[17] The fraction of **1** with respect to the total ions at *m/z* 1044 was found to depend on the reaction conditions adopted for the synthesis. At typically low temperatures and a constant relative amount of iodosylbenzene, as described in the Experimental Section, the amount of the oxo iron species was never below 60%. Furthermore, with all the amines assayed in the present study, the isomeric $[(TPFPP)^{\bullet+}Fe^{IV}{=}O]^+$ and $[(TPFPP{+}O)Fe^{III}]^+$ complexes proved to be readily discriminated by their distinct reactivities. The careful scrutiny of the reactivity patterns with both the NO probe and the sampled amine provided in all cases an overall consistent picture of their ion chemistry.

Oxidation of Gaseous Amines by $[(TPFPP)^{\bullet+}Fe^{IV}{=}O]^+$ Ions. When ions **1** obtained by ESI are conveyed into the FT-ICR cell, mass selected, and allowed to react with a stationary concentration of tertiary amines (A), three ionic products may be observed (eq 4a−c). The first one is the product of electron

$$\underset{\mathbf{1}}{[(TPFPP)^{\bullet+}Fe^{IV}{=}O]^+} + A \longrightarrow \begin{cases} \xrightarrow{ET} A^{\bullet+} + (TPFPP)Fe^{IV}{=}O & (4a) \\ \xrightarrow{HT} [A(-H)]^+ + (TPFPP)Fe^{III}(OH) & (4b) \\ \xrightarrow{OAT} [(TPFPP)Fe^{III}]^+ + A(O) & (4c) \\ \xrightarrow{HAT} \text{X} [(TPFPP)Fe^{IV}(OH)]^+ + [A(-H)]^{\bullet} & (4d) \end{cases}$$

transfer (ET), namely the radical cation of the amine ($A^{\bullet+}$), implying the concomitant formation of neutral $(TPFPP)Fe^{IV}{=}O$. A second product derives from a formal hydride transfer (HT) process producing $[A(-H)]^+$ ions (iminium ions, the $[A(-H)]^+$ notation indicates the species obtained from A by hydride loss) and neutral $(TPFPP)Fe^{III}(OH)$. This reaction was found to proceed by a multistep sequence to be discussed in a following section. The third process releases $[(TPFPP)Fe^{III}]^+$ ions, implying an oxygen atom transfer to the amine (OAT). A formal ligand addition product is observed as well. Upon close inquiry, however, the origin of this product can be traced to the reaction of the isobaric $[(TPFPP{+}O)Fe^{III}]^+$ species (eq 5) which can obviously not be differentiated by the mass selection routines of FT-ICR mass spectrometry.

$$[(TPFPP{+}O)Fe^{III}]^+ + A \longrightarrow [(TPFPP{+}O)Fe(A)]^+ \quad (5)$$

This conclusion is supported by several lines of evidence. The ligand addition reactivity is well documented for tetracoordinate ferric porphyrin ions such as $[(TPFPP)Fe^{III}]^+$ ions[11] (as found characteristic of the NO reaction with the porphyrin oxidized $[(TPFPP{+}O)Fe^{III}]^+$ isomer). Notably, the extent of amine addition is quantitatively matched by the fraction of nitrosyl adduct formed from the same sampled ion population. This outcome is expected from an ion mixture where the relative amount of $[(TPFPP{+}O)Fe^{III}]^+$ isomer remains constant during the time of the experimental assay, displaying the characteristic ligand addition reactivity toward both NO and amines. Further evidence pointing to coordination of the amine to a vacant axial site on the metal comes from CID experiments activating the $[(TPFPP{+}O)Fe^{III}(A)]^+$ adduct toward dissociation. The exclusive loss of the intact amine is observed. No evidence is found for the possible formation of an oxidized amine product within the complex. This behavior is clearly different from the reactivity displayed by the active oxidant **1** with pyridine, reported previously.[11] In this case the pyridine adduct showed clear evidence of pyridine-O bond formation, releasing a formal [pyridine(O)] unit both when activated to CID or when allowed to undergo a ligand substitution process. The collective evidence gathered on the reactivity toward amines, including trialkylamines, *N*-phenylpyrrolidine, piperidine, and *N*,*N*-dimethylanilines, showed a uniform behavior whereby **1** ions yield ET, HT, and OAT products and $[(TPFPP{+}O)Fe^{III}]^+$ ions yield the corresponding adducts. The latter species are not of primary interest. Their contribution to the overall pattern causes little interference and can be subtracted with no consequence whatsoever. Thus their reactions will not be further discussed.

In no instance is an HAT product, retaining the charge on the iron porphyrin complex, ever observed. If formed, this species, corresponding to $[(TPFPP)Fe^{IV}(OH)]^+$ ions with a formal protonated ferryl unit, would appear at *m/z* 1045 (eq

Table 1. Kinetic Data for the Gas-Phase Reaction of $[(TPFPP)^{\bullet+}Fe^{IV}{=}O]^+$ with Tertiary Amines (A)[a]

			product distribution[e] (%)		
A (IE)[b]	k_{exp}[c]	ϕ[d]	ET	HT	OAT
$(CH_3)_3N$ (7.85)	0.44	4.5		100	
$(C_2H_5)_3N$ (7.53)	1.4	14	15	85	
c-$C_4H_8N{-}C_6H_5$[f] (6.8)	1.1	8.9	30	70	
c-$C_5H_{10}NH$[g] (8.03)	0.3	2.7		100	
p-$CH_3{-}C_6H_4N(CH_3)_2$ (6.93)	1.2	11	44	40	16
$C_6H_5N(CH_3)_2$ (7.12)	0.8	6.0	33	67	
p-$F{-}C_6H_4N(CH_3)_2$ (7.5)	0.7	5.3	55	45	
p-$Br{-}C_6H_4N(CH_3)_2$ (7.3)	0.7	5.5	55	27	18
p-$CF_3{-}C_6H_4N(CH_3)_2$ (n.a.)	0.3	2.1	10	48	42
$C_6F_5N(CH_3)_2$ (8.5, vertical)	1.0	7.0			100

[a] Reactions were run at least in triplicate at the temperature of the FT-ICR cell of 300 K, and averaged results are presented. Piperidine, a secondary amine, is also included. [b]Ionization energies (IE)[23] in eV are given in parentheses (n.a. stands for not available). [c]Second-order rate constants in units of 10^{-10} cm^3 molecule^{-1} s^{-1}. The estimated error is ±30%, while the internal consistency of the data is within ±10%. [d]Reaction efficiency, $\phi = k_{exp}/k_{coll} \times 100$. Collision rate constants (k_{coll}) evaluated with the parametrized trajectory theory.[16] [e]Product branching resulting from electron transfer (ET), hydride loss (HT), and oxygen atom transfer (OAT) channels. [f]*N*-Phenylpyrrolidine. [g]Piperidine.

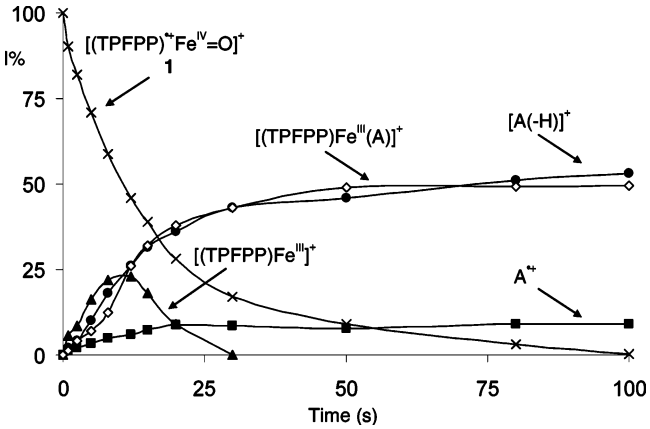

Figure 3. Time dependence of relative ion intensities (*I*%) following the selection of **1** in the FT-ICR cell and allowing it to react with *p*-$CF_3{-}C_6H_4N(CH_3)_2$ (A) at 2.3×10^{-8} mbar.

4d). Thus, with reference to Scheme 1, from a first inspection of this gas-phase reaction, an ET process is clearly discernible whereas an HAT path is not emerging.

The product distribution and the kinetic data for the reaction of **1** with amines are summarized in Table 1. The second-order rate constants for the overall reaction of **1** are reported together with the reaction efficiencies ($\phi = k_{exp}/k_{coll} \times 100$), measuring the fraction of reactive collisions. In other words, ϕ yields the percent number of collision events leading to products and is obtained from the ratio of the experimental rate constant, k_{exp}, and the rate for ion-neutral collision, k_{coll}, calculated by parametrized trajectory theory.[16] The progress of the reaction is recorded by means of ion abundance versus time plots such as the one depicted in Figure 3. For the sake of clarity, the contribution of $[(TPFPP{+}O)Fe^{III}]^+$ and the ensuing ligand addition product are omitted. The distinct pathways of eqs 4a−c appear to be parallel and independent, leading to ET, HT, and OAT products in ion abundance ratios that remain constant with elapsed time. The $[(TPFPP)Fe^{III}]^+$ product ion of the OAT channel, in the presence of neutral A, undergoes an addition process, conforming to the usual reactivity behavior of porphyrin iron(III) ions with gaseous amines.

Typically, two or more channels are active for the amines listed in Table 1. Notable exceptions are trimethylamine and piperidine (a secondary amine), yielding only an HT product, and $C_6F_5N(CH_3)_2$ which reacts only by the OAT pathway. Interestingly, these three amines are the only ones in the table that do not show any radical cation formation (ET). This finding appears related to the comparatively higher ionization energies of these neutrals. The experimental IE values from the NIST database (also listed in Table 1) seem to indicate an onset for the formation of the ET product. The amine radical cation appears in fact only for IE values ≤7.53 eV, suggesting that the ET process may otherwise be endothermic. From this evidence, an approximate lower limit of 7.5 eV for the IE value of $[(TPFPP)Fe^{IV}{=}O]$ in the gas phase is inferred. The formation of an HT product by a direct path starting from the reagents, **1**, and A (as described in eq 6, path c) is not only consistent with the observed kinetics but also conceivable on thermochemical grounds. An alternative possibility that the amine radical cation, formed by ET and released free in the gas phase, may be a precursor of $[A(-H)]^+$ ions (paths a → b, in eq 6) is in fact hardly compatible with an appearance energy of the iminium ion that is substantially higher than the IE value of the parent amine.[23,24] This conclusion obviously holds also in those cases, as in the trimethylamine reaction, where the release of an $A^{\bullet+}$ product is not accessed and the formation of the iminium ion (path 6c) may still be thermochemically allowed within the ion neutral complex **2** (eq 6), driven by the concomitant formation of neutral $(TPFPP)Fe^{III}(OH)$. Therefore, the point that $[A(-H)]^+$ product ions do not proceed by the formation of free $A^{\bullet+}$ does not exclude a stepwise mechanism, whereby the same collision complex (**2**) accounts for the formation of both $A^{\bullet+}$ and $[A(-H)]^+$, as further discussed in a next section. However,

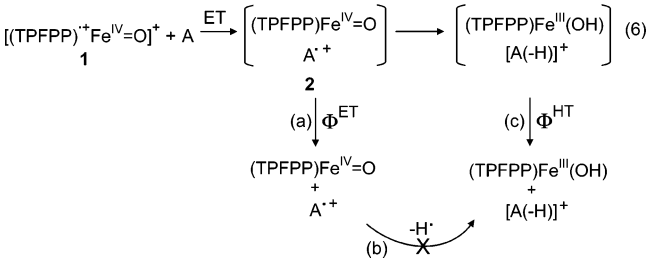

while a high IE prevents the formation of the free amine radical cation both for aliphatic and aromatic amines, their oxidation products are different. HT product ions are obtained from the former and an OAT path is prevailing for the latter.

A View into the Mechanism of Oxidation of *N*,*N*-Dimethylanilines by $[(TPFPP)^{\bullet+}Fe^{IV}{=}O]^+$. The *N*,*N*-dimethylanilines represent a useful series of structurally similar compounds whose electronic properties at the reaction center may be modulated by varying the substituents on the aromatic ring. Accordingly, such a series have been studied in solution with regard to their oxidative dealkylation by both monooxygenase enzymes and model compounds.[2,3,5,6a,25] Among the paths depicted in eq 4, the formation of the aniline based ions, namely

(23) Hunter, E. P.; Lias, S. G. *NIST Chemistry Webbook*, NIST Standard Reference Database Number 69; Linstrom, P. J., Mallard, W. G., Eds.; National Institute of Standards and Technology: Gaithersburg, MD, 2005; http://webbook.nist.gov.
(24) Traeger, J. C. *J. Phys. Chem. A* **2007**, *111*, 4643.

Table 2. Kinetic and Computed Thermodynamic Data for the Reaction of $[(TPFPP)^{\bullet+}Fe^{IV}{=}O]^{+}$ with *N*,*N*-Dimethylanilines ($ArN(CH_3)_2$)

$ArNMe_2$	$\phi^{ET}+\phi^{HT\,a}$	$BDE^{b,c}$ ($>NCH_2$-H)	IE^b
p-CH_3-$C_6H_4N(CH_3)_2$	9.2	355 (376)	6.81
$C_6H_5N(CH_3)_2$	6.0	356 (334,383)	7.04
p-F-$C_6H_4N(CH_3)_2$	5.3	358	7.11
p-Br-$C_6H_4N(CH_3)_2$	4.5	359	7.07
p-CF_3-$C_6H_4N(CH_3)_2$	1.3	360 (385)	7.52
$C_6F_5N(CH_3)_2$	-	361	7.82

[a] $\phi^{ET}+\phi^{HT}$ is the sum of the efficiencies for the formation of the ET and HT products, obtained from data reported in Table 1, at 300 K. [b]BDE (in kJ mol^{-1}) for the α C−H bond in the neutral *N*,*N*-dimethylanilines and IE (eV) of the neutral aniline were determined at B3LYP/6-311+G** level, including zero point vibrational energy corrections. [c]Experimental values[26] are reported in parentheses.

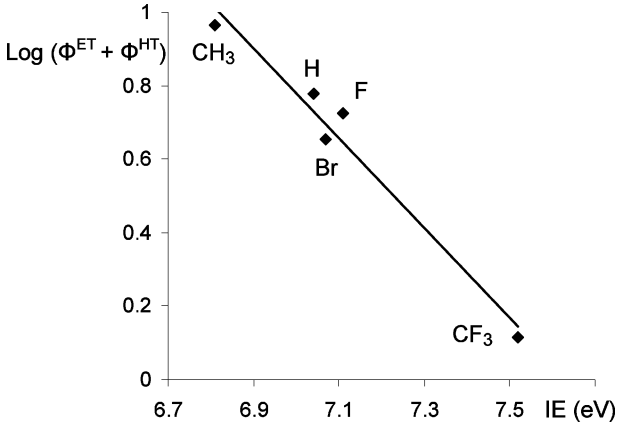

Figure 4. Plot of $\log(\phi^{ET}+\phi^{HT})$ (where $\phi^{ET}+\phi^{HT}$ is the sum of the reaction efficiencies for the ET and HT channels) as a function of the IE for the reactant *p*-X-substituted *N*,*N*-dimethylaniline (X is given for each datum on the plot).

the amine radical cation (4a) and the formal hydride abstraction product or iminium ion (4b), is more easily accounted for. The finding that the two paths appear in parallel, with no evidence of intervening free intermediates, may be explained by a mechanism initiated by an ET step leading to a complex (**2** in eq 6) that may either dissociate to give the aniline radical cation or proceed by further reaction to form the iminium ion. Overall these pathways depend on an ET event and are thus expected to depend on the IEs of the neutral anilines. Because experimental IEs are available only in part for the tested *N*,*N*-dimethylanilines, computational data have been acquired and are listed in Table 2 together with the computed values of the C−H bond dissociation energy (BDE) for the methyl group α to the amino nitrogen. The first column in Table 2 reports the sum of the efficiencies for the formation of the ET and HT products ($\phi^{ET}+\phi^{HT}$) which decreases along a trend of increasing IEs. The relationship between $\phi^{ET}+\phi^{HT}$ and the computed IE values is illustrated in the plot of Figure 4 where the data are fitted by a straight line. As shown in Table 1, the partition into the two products is not a simple function of the electronic properties of the anilines, at least as described by their IE values, although the least oxidizable *p*-trifluoromethyl compound (among the ones still reacting by ET/HT) shows the smallest release of the radical cation product.

As the formation of the amine radical cation becomes endothermic, which is likely occurring with $C_6F_5N(CH_3)_2$, the OAT path takes over, making the reaction of this amine a relatively efficient process ($\phi = 7.0$, Table 1). If this reaction were conforming to an ET initiated process, $C_6F_5N(CH_3)_2$, owning the highest IE, should behave as the least reactive among the probed *N*,*N*-dimethylanilines. However, also invoking an HAT initiated process, proceeding by a "rebound" step, one should not expect an enhanced reactivity in view of the similar BDEs for the α C−H bond in the aniline series,[26] as also shown by the computed data reported in Table 2. So, also this possible mechanism does not explain the relatively higher reactivity of $C_6F_5N(CH_3)_2$. Indeed, in recent, thorough theoretical studies[27] of the α C−H activation of *N*,*N*-dimethylanilines with a Compound I model endowed with an SH axial ligand, it is found that the hydrogen atom abstraction is the rate-limiting step of the hydroxylation reaction leading to a carbinolaniline intermediate. These studies, however, provide an interpretation of the several facets of the enzymatic oxidation of anilines in terms of a two-state reactivity model.[28] In particular, in a series of para-substituted *N*,*N*-dimethylanilines, as the substituent becomes more electron withdrawing the reactivity pattern moves from spin-selective to two-state reactivity. In the presence of a para-NO_2 group, a substantial fraction of the reaction proceeds via the high spin quartet besides the lower energy low spin doublet route. While the NO_2-substituted aniline could not be sampled due to its scant volatility, it is possible that the gas-phase reactivity behavior of $C_6F_5N(CH_3)_2$ toward **1** may similarly reflect a switch to two-state reactivity. The formation of a carbinolaniline as the primary hydroxylation product formed within the collision complex would also be in agreement with the small binding energy calculated for the association of this species to the heme in both the doublet and the quartet energy profile.[27] In contrast, the formation of an amine *N*-oxide is expected to yield a stable adduct, based on the evidence from the pyridine reaction likely forming this species, as mentioned previously. Thus, the formation of an aniline *N*-oxide as an OAT product does not seem to be occurring under the present conditions.[1e,29] In this context, recent theoretical studies, aimed at modeling the generation of active species of cytochrome P450 from different precursors and the ensuing oxidative N-demethylation of *N*,*N*-dimethylanilines, have investigated the detailed pathway leading to the high valent oxo iron intermediate, using *N*,*N*-dimethylaniline-*N*-oxide as an oxygen atom donor, along the possible different spin state surfaces.[30] From

(25) (a) Dowers, T. S.; Rock, D. A.; Rock, D. A.; Jones, J. P. *J. Am. Chem. Soc.* **2004**, *126*, 8868. (b) Bhakta, M. N.; Wimalasena, K. *Eur. J. Org. Chem.* **2005**, 4801.
(26) Dombrowski, G. W.; Dinnocenzo, J. P.; Farid, S.; Goodman, J. L.; Gould, I. R. *J. Org. Chem.* **1999**, *64*, 427−431.
(27) (a) Li, C.; Wu, W.; Kumar, D.; Shaik, S. *J. Am. Chem. Soc.* **2006**, *128*, 394. (b) Wang, Y.; Kumar, D.; Yang, C.; Han, K.; Shaik, S. *J. Phys. Chem. B* **2007**, *111*, 7700.
(28) (a) Shaik, S.; Hirao, H.; Kumar, D. *Acc. Chem. Res.* **2007**, *40*, 532. (b) Shaik, S.; de Visser, S. P.; Ogliaro, F.; Schwarz, H.; Schröder, D. *Curr. Opin. Chem. Biol.* **2002**, *6*, 556. (c) Schröder, D.; Shaik, S.; Schwarz, H. *Acc. Chem. Res.* **2000**, *33*, 139. (d) Shaik, S.; Filatov, M.; Schroder, D.; Schwarz, H. *Chem.—Eur. J.* **1998**, *4*, 193.
(29) Guengerich, F. P.; Muller-Enoch, D.; Blair, I. A. *Mol. Pharmacol.* **1986**, *30*, 287.
(30) Cho, K.-B.; Moreau, Y.; Kumar, D.; Rock, D. A.; Jones, J. P.; Shaik, S. *Chem.—Eur. J.* **2007**, *13*, 4103.

these data, still regarding the Compound I model endowed with an SH axial ligand, it may be observed that the OAT reaction between the Compound I model and *N*,*N*-dimethylaniline leading to *N*,*N*-dimethylaniline-*N*-oxide is exothermic by ca. 24 kJ mol^{-1}. However, the reaction pathway proceeds by a transition state lying comparatively high in energy, implying activation energy barriers greater than 50 kJ mol^{-1}.[30] Altogether, the computational results concur in suggesting that the formation of an N-oxide as the product of the OAT process is highly unlikely.

Kinetic Isotope Effects in the Oxidation of *N*,*N*-Dimethylanilines by [(TPFPP)$^{\bullet+}$Fe^{IV}=O]$^+$ Ions. In the several studies addressing the oxidative N-dealkylation of *N*,*N*-dimethylaniline catalyzed by cytochromes P450 and iron porphyrin complexes, the hydrogen/deuterium kinetic isotope effect (KIE) has largely been exploited as a mechanistic tool.[3,5,6,25,27] The same probe is used in the present study to gain an insight into the gas-phase reaction pathway. In fact, while the observed ionic products, the amine radical cation and the iminium ions, testify an ET initiated reaction, the path leading to the iminium ion (overall, a formal HT product) from the intermediate ion-neutral complex (**2** in eq 7) may be envisioned as either a concerted hydrogen atom transfer (HAT) or a stepwise proton transfer (PT) and electron transfer (ET) route. The occurrence

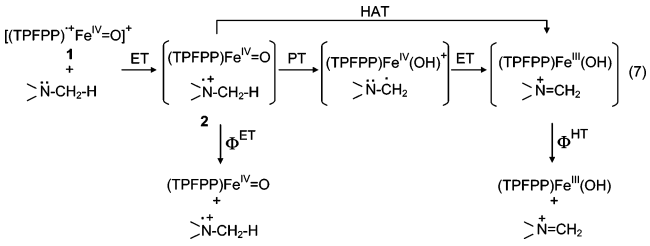

of a PT event is conceivable in view of the pronounced acidity of *N*,*N*-dimethylaniline radical cations[5c] and of the basic properties of the iron(IV)−oxo group.[5b,c,31] In particular, the (TPFPP)Fe^{IV}=O ferryl species is estimated to be more basic than pyridine.[5b,c] Assuming the same relative basicity to hold in the gas phase, a PA value ≥ 930 kJ mol^{-1} is derived.[23] The PA values of the radicals representing the conjugate bases of the *N*,*N*-dimethylaniline radical cations, as obtained by calculations at the B3LYP/6-311+G** level, provide a homogeneous set of data listed in Table 3. The *N*-methyl-*N*-arylaminomethyl radicals so obtained by deprotonation of the aniline radical cations are expected to be easily oxidized to the iminium ion, in view of their low IE values, also listed in Table 3.

Finally, Table 3 provides also the computed values of the C−H bond dissociation energy for the methyl group α to the amino nitrogen in the *N*,*N*-dimethylaniline radical cations. The computed thermochemical data provide a basis to survey the KIE affecting the formation of the iminium ion. To this end the reaction of *N*,*N*-bis(dideuteriomethyl)anilines was investigated. The use of substrates with partial labeling in both methyl groups was preferred, relative to *N*-methyl *N*-(trideuteriomethyl)-anilines, where a masking effect may arise if the rotation of CH_3 and CD_3 groups around the C(aromatic)−N bond is slower than hydrogen or proton transfer, an event found to affect the reaction occurring within an enzyme pocket.[3b,5f] When *N*,*N*-bis(dideuteriomethyl)anilines are allowed to react with **1**, the HT path yields two products implying formal H$^-$ and D$^-$ abstraction from the amine methyl groups.[32] The ion intensity ratio of the so-formed species, [A(−H)]$^+$ and [A(−D)]$^+$, is time independent and, corrected by a statistical factor (eq 8), yields the KIE values reported in Table 3.

Table 3. Kinetic Isotope Effects for the HT Path in the Reaction of [(TPFPP)$^{\bullet+}$Fe^{IV}=O]$^+$ with *N*,*N*-Bis(dideuteriomethyl)anilines (ArN(CHD$_2$)$_2$) and Computed Thermodynamic Data

ArNMe$_2$	KIE[a]	BDE[b] (>N^{+}CH$_2$-H)	PA[b] (>NCH$_2^{\bullet}$)	IE[b] (>NCH$_2^{\bullet}$)
p-CH$_3$-C$_6$H$_4$N(CHD$_2$)$_2$	2.4	239	1016	5.61
C$_6$H$_5$N(CHD$_2$)$_2$	2.7	229	995	5.72
p-F-C$_6$H$_4$N(CHD$_2$)$_2$	2.8	234	990	5.83
p-Br-C$_6$H$_4$N(CHD$_2$)$_2$	3.5	241	993	5.86
p-CF$_3$-C$_6$H$_4$N(CHD$_2$)$_2$	5.0	223	952	6.10
C$_6$F$_5$N(CHD$_2$)$_2$	n.a.	216	924	6.31

[a] KIE values obtained according to eq 8; n.a. stands for not available. [b] BDE (in kJ mol^{-1}) for the α C−H bond in the radical cation of *N*,*N*-dimethylanilines, PA (in kJ mol^{-1}) for the *N*-methyl-*N*-arylaminomethyl radical (namely the conjugate base of the *N*,*N*-dimethylaniline radical cation), and IE (eV) for the *N*-methyl-*N*-arylaminomethyl radical were determined for the unlabeled compounds at the B3LYP/6-311+G** level, including zero-point vibrational energy corrections.

$$\mathrm{KIE} = 2 \times \frac{I[\mathrm{A}(-\mathrm{H})]^+}{I[\mathrm{A}(-\mathrm{D})]^+} \qquad (8)$$

The KIE values increase as the para substituent changes from an electron donor (CH_3) to an electron withdrawing group (CF_3). The trend is paralleled by the decrease in the PA of the *N*-methyl-*N*-arylaminomethyl radical. Both the magnitude of the KIE values, indicative of a primary KIE, and their variation with the PA of the conjugate base of the aniline radical cation (computed values are listed in Table 3) are consistent with the operation of a KIE affecting the PT step of eq 7. In fact, based on the relative PA values, the KIE increases as the PA of the *N*-methyl-*N*-arylaminomethyl radical approaches the estimated PA of the iron(IV)-oxo group (PA ≥ 930 kJ mol^{-1}) and the PT reaction approaches thermoneutrality, in agreement with the Melander−Westheimer KIE model.[33] In contrast, in the event of a concerted HAT reaction one may expect the magnitude of the KIE values to scale with the BDE(C−H) for the methyl group α to the amino nitrogen in the aniline radical cation. However, a clear trend should not result for the measured KIEs in this case, based on the somewhat uniform values of the relative BDE(C−H) (Table 3). The KIE data appear then to

(31) (a) Green, M. T.; Dawson, J. H.; Gray, H. B. *Science* **2004**, *304*, 1653. (b) Behan, R. K.; Hoffart, L. M.; Stone, K. L.; Krebs, C.; Green, M. T. *J. Am. Chem. Soc.* **2006**, *128*, 11471. (c) Behan, R. K.; Green, M. T. *J. Inorg. Biochem.* **2006**, *100*, 448. (d) Horner, O.; Mouesca, J.-M.; Solari, P. L.; Orio, M.; Oddou, J.-L.; Bonville, P.; Jouve, H. M. *J. Biol. Inorg. Chem.* **2007**, *12*, 509. (e) Alfonso-Prieto, M.; Borovik, A.; Carpena, X.; Murshudov, G.; Melik-Adamyan, W.; Fita, I.; Rovira, C.; Loewen, P. C. *J. Am. Chem. Soc.* **2007**, *129*, 4193. (f) Rovira, C. *ChemPhysChem* **2005**, *6*, 1820. (g) Silaghi-Dumitrescu, R. *J. Biol. Inorg. Chem.* **2004**, *9*, 471.

(32) The possibility of a ring hydrogen being removed from the radical cation of an aromatic compound, owning alternative acidic sites on a ring substituent, has been discarded in previous studies using appropriately labelled compounds. (a) Chiavarino, B.; Crestoni, M. E.; Fornarini, S. *Chem. Phys. Lett.* **2003**, *372*, 183. (b) Baciocchi, E.; Bietti, M.; Chiavarino, B.; Crestoni, M. E.; Fornarini, S. *Chem.—Eur. J.* **2002**, *8*, 532.

(33) (a) Westheimer, F. H. *Chem. Rev.* **1961**, *61*, 265. (b) Melander, L.; Saunders, W. H. *Reaction Rates of Isotopic Molecules*; Krieger Publishing Company: Malabar, 1987.

favor a stepwise pathway to the iminium ion, comprising a PT event followed by the fast oxidation of the so-formed *N*-methyl-*N*-arylaminomethyl radical. In a related context, it may be relevant to note, however, that HAT reactions are a topic of intensive study. The reaction of an exemplary hydrogen abstractor, the *tert*-butoxyl radical, was found to display rates that are rather entropy- than enthalpy-controlled for substrates with relatively low C−H bond dissociation energy.[34] Regarding the Cytochrome P450 catalyzed *N*-demethylation, the KIE associated to HAT from neutral *N*,*N*-dimethylanilines has been accounted for in terms of electronic substituent effects on the reaction barrier and of two-state reactivity.[3f,27b] In the theoretical study on a compound I model of Cytochrome P450 it is in fact shown that both low- and high-spin states may contribute to the overall reactivity when strongly electron withdrawing substitutents such as cyano or nitro groups are present on the aromatic ring.[27b]

A Parallel with the Gas-Phase Oxidation of Aromatic Amines by Bare FeO^+. In the quest for simplified models for the high valent oxo iron species in the active sites of heme enzymes, the most essential model system is the bare FeO^+ cation, which has been generated and extensively studied in the gas phase.[35,10f] The dissociation of metastable FeO^+ complexes formed with *N*-methylaniline upon chemical ionization revealed a dehydration process leading to an imine/Fe^+ complex,[36] potentially an intermediate to carbinolamine formation in an aqueous environment. The bimolecular reactivity of FeO^+ with *N*,*N*-dimethylaniline was also studied by FT-ICR displaying remarkably similar facets with respect to the reaction of **1** that is presently reported.[36] The major product ions are in fact the amine radical cation (70%) and an iminium ion by a formal hydride transfer reaction (30%). The KIE affecting the latter process was obtained by the reaction with *N*-methyl-*N*-(trideuteriomethyl)aniline. The KIE proved to be sensitive to the presence and electronic properties of a ligand, increasing from 2.0 for bare FeO^+ to 2.6 and 3.0 for $(L)FeO^+$ with $L = C_6H_6$ and C_6H_5CN, respectively, thus coming to a close, though probably fortuitous, agreement with the KIE displayed by **1**, where the oxo iron unit is embedded in the porphyrin coordination environment.

However, a unifying feature for the reaction of *N*,*N*-dimethylaniline with both FeO^+ and **1** is the ET step as the initial elementary step in the gas-phase oxidation. The ET step is permitted to FeO^+ by the notably high IE(FeO) of 8.9 eV and appears to be allowed to **1** as well. Comparably important is the C−H bond activation leading to the formation of an iminium ion, a possible central intermediate in the N-dealkylation process in the condensed phase.

Conclusions

A high-valent iron(IV) oxo porphyrin cation radical complex, **1**, has been prepared and characterized in the gas phase, providing a model for the high valent oxo iron intermediates commonly referred to as Compound I species in biological contexts. The gas phase may grant an extreme simplification relative to the complex environment of the heme group within the enzyme pocket, which is known to markedly affect the reactivity of the catalytically active species.[37] The mass spectrometric study of the reactivity of naked **1** with gaseous amines has thus unveiled elementary pathways that could only be inferred in condensed phase studies where mechanistic information typically relied on the analysis of the neutral end products. The major relevant information thus gained may be summarized in the following points. The reaction is initiated by an ET event for the majority of the tested amines which included tertiary aliphatic and aromatic amines as well as a cyclic and a secondary amine. For a series of *N*,*N*-dimethylanilines the reaction efficiency for the ET activated pathways was found to correlate with the IE of the base. It is then implied that the ET process is allowed to occur, at least within the ion neutral complex formed upon the encounter of **1** with the amine, in line with the pronounced oxidizing power of **1**, which is due in part to the electron deficient character of the porphyrin ligand.[6b,38] An important factor is also the lack of an axial ligand in the pentacoordinate complex **1**. Indeed, theoretical calculations have investigated a Compound I model where the heme is represented by an iron−porphine complex and an SH group replaced the axial cysteine ligand which is present in P450, showing that the reaction with *N*,*N*-dimethylaniline proceeds by an HAT mechanism.[27] However, the same authors find that on removing the SH ligand the reaction pathway turns to initial spontaneous ET from the aniline, followed by proton abstraction.[39] The same stepwise pathway is presently inferred from the kinetic study of the reaction of naked **1** with a series of *N*,*N*-dimethylanilines. The primary ET event, yielding complex **2**, may either release the amine radical cation ($A^{\bullet+}$) or proceed by proton transfer from the acidic methyl groups of $A^{\bullet+}$ to the iron(IV)−oxo group. Accordingly, the PT process is characterized by a KIE that increases as the PA of the conjugate base, the *N*-methyl-*N*-arylaminomethyl radical ($A(-H)^{\bullet}$), decreases and the reaction approaches thermoneutrality. The so-formed radical is finally oxidized to the iminium ion. The reaction of **1** with $C_6F_5N(CH_3)_2$, the amine owning the highest IE in the *N*,*N*-dimethylaniline series, presents unique reactivity features, that may only in part be accounted for by the fact that the ET route has become thermodynamically unfavorable. The observed relatively high efficiency of the OAT pathway,

(34) (a) Tanko, J. M.; Friedline, R.; Suleman, N. K.; Castagnoli, N. *J. Am. Chem. Soc.* **2001**, *123*, 5808. (b) Finn, M.; Friedline, R.; Suleman, N. K.; Wohl, C. J.; Tanko, J. M. *J. Am. Chem. Soc.* **2004**, *126*, 7578.
(35) (a) Jackson, T. C.; Jacobson, D. B.; Freiser, B. S. *J. Am. Chem. Soc.* **1984**, *106*, 1252. (b) Schroeder, D.; Schwarz, H. *Angew. Chem., Int. Ed. Engl.* **1990**, *29*, 1433. (c) Schroeder, D.; Schwarz, H. *Angew. Chem., Int. Ed. Engl.* **1990**, *29*, 1431. (d) Fiedler, A.; Schroeder, D.; Shaik, S.; Schwarz, H. *J. Am. Chem. Soc.* **1994**, *116*, 10734. (e) Clemmer, D. E.; Chen, Y.-M.; Khan, F. A.; Armentrout, P. B. *J. Phys. Chem.* **1994**, *98*, 6522. (f) Baranov, V.; Javahery, G.; Hopkinson, A. C.; Bohme, D. K. *J. Am. Chem. Soc.* **1995**, *117*, 12801. (g) Schroeder, D.; Schwarz, H.; Clemmer, D. E.; Chen, Y.; Armentrout, P. B.; Baranov, V.; Bohme, D. K. *Int. J. Mass Spectrom. Ion Processes* **1997**, *161*, 175. (h) Broenstrup, M.; Schroeder, D.; Schwarz, H. *Chem.−Eur. J.* **1999**, *5*, 1176.
(36) Broenstrup, M.; Schroeder, D.; Schwarz, H. *Can. J. Chem.* **1999**, *77*, 774.
(37) Watanabe, Y.; Nakajima, H.; Ueno, T. *Acc. Chem. Res.* **2007**, *40*, 554.
(38) (a) Goh, Y. Mee; Nam, W. *Inorg. Chem.* **1999**, *38*, 914. (b) Dolphin, D.; Traylor, T. G.; Xie, L. Y. *Acc. Chem. Res.* **1997**, *30*, 251.
(39) Supplementary material in ref 30.
(40) de Visser, S. P.; Shaik, S.; Sharma, P. K.; Kumar, D.; Thiel, W. *J. Am. Chem. Soc.* **2003**, *125*, 15779.
(41) (a) Newcomb, M.; Toy, P. H. *Acc. Chem. Res.* **2000**, *33*, 449. (b) Pan, Z.; Zhang, R.; Newcomb, M. *J. Inorg. Biochem.* **2006**, *100*, 524. (c) Harischandra, D. N.; Zhang, R.; Newcomb, M. *J. Am. Chem. Soc.* **2005**, *127*, 13776. (d) Dey, A.; Ghosh, A. *J. Am. Chem. Soc.* **2002**, *124*, 3206. (e) Koppenol, W. H. *J. Am. Chem. Soc.* **2007**, *129*, 9686. (f) Collman, J. P.; Chien, A. S.; Eberspacher, T. A.; Brauman, J. I. *J. Am. Chem. Soc.* **2000**, *122*, 11098. (g) Song, W. J.; Ryu, Y. O.; Song, R.; Nam, W. *J. Biol. Inorg. Chem.* **2005**, *10*, 294.

forming a carbinolamine product, may rather suggest the incursion of a mechanism along a route of different spin multiplicity.

It is worth noting, however, that the mechanistic pathway displayed by **1** in the activation of gaseous amines may constitute a representation of what happens in enzymes like horseradish and lignin peroxidase,[2d,5c,d] where the Compound I species is a much better electron acceptor than the corresponding intermediate of P450.[40]

In conclusion, the oxidation of amines by **1** studied in the gas phase, by viewing directly the charged intermediates and their temporal evolution, may provide an ultimate archetype against which the intriguingly complex behavior of Compound I intermediates and model complexes in condensed phases[1−6,41] may be fruitfully compared.[8]

Acknowledgment. This project was supported by the Università di Roma "La Sapienza" and by the Italian Ministero dell'Università e della Ricerca.

JA077286T